2023

Analysis of Degradation of Sb2Se3 Thin Film Solar Cells Deploying a Time-Dependent Approach Linked with 1D-AMPS Simulation

Ming-Lang Tseng

Malek Gassoumi

Nima Ghadiri

Results in Physics 53 (2023) 107043

Contents lists available at ScienceDirect

Results in Physics

journal homepage: www.elsevier.com/locate/rinp

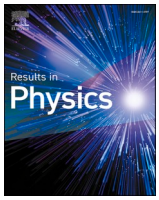

Analysis of degradation of Sb_2Se_3 thin film solar cells deploying a time-dependent approach linked with 1D-AMPS simulation

Ming-Lang Tseng [a,b], Malek Gassoumi [c], Nima E. Gorji [d,*]

[a] Institute of Innovation and Circular Economy, Asia University, Taiwan
[b] Department of Medical Research, China Medical University Hospital, China Medical University, Taichung, Taiwan
[c] Laboratory of Condensed Matter and Nanosciences, University of Monastir, Monastir 5000, Tunisia
[d] Mechatronic Engineering, Technological University Dublin, Dublin 15, Ireland

ARTICLE INFO

Keywords:
Degradation
Sb_2Se_3
Defect accumulation
Thin films
Solar cells
AMPS-1D

ABSTRACT

In this paper, we have developed a time-dependent model to study defect growth in the absorber layer of Sb_2Se_3 thin film solar cells. This model has been integrated with the AMPS-1D simulation platform to investigate the impact of increasing defect density at different positions within the Sb_2Se_3 layer on the electrical parameters of the solar cell. We adopted the Gloeckler standard model for thin films in AMPS to represent Sb_2Se_3 materials. The study focuses on tracking the degradation of device performance parameters as donor-like mid-gap states accumulate in the Sb_2Se_3 layer over time. We monitored the variation of key electrical parameters, including efficiency (η), fill factor (*FF*), open-circuit voltage (V_{oc}), and short-circuit current (J_{sc}), at three different positions: the interface with CdS, the bulk of the Sb_2Se_3 layer, and the interface with the top contact. These positions are susceptible to increasing defect density during prolonged operation and irradiation. To pinpoint the most sensitive part of the Sb_2Se_3 layer to defect accumulation, we divided the layer into three sub-layers. Our simulation results highlight that the CdS/Sb_2Se_3 interface is the most vulnerable position in the cell when it comes to defect accumulation. The practical implication of this study is that special attention should be given to the CdS/Sb_2Se_3 interface during material deposition and the development of high-stability Sb_2Se_3 thin film solar cells.“

Introduction

Thin film solar cells have emerged as a promising and cost-effective alternative to traditional silicon-based solar cells. However, technological advances have not been able to mitigate the degradation of thin film solar cells. This degradation can occur due to a range of factors, including exposure to moisture, temperature fluctuations, and the presence of impurities or defects in the film [1,2]. Several studies have shown that the performance of thin film solar cells can degrade significantly over time, leading to decreased power output and reduced efficiency [3,4]. Therefore, understanding the mechanisms behind the degradation of thin film solar cells is crucial for improving their durability and longevity. To address the degradation of thin film solar cells, researchers have explored various strategies. These include the development of emerging materials with improved stability, such as perovskites, metal-oxides, and Sb2Se3 materials [5,6]. Another approach is the use of protective coatings and encapsulation techniques to shield the cells from external factors. Several solutions have been suggested for mitigating the degradation of Sb_2Se_3 thin film solar cells. One of the most recent absorber options, antimony selenide (Sb_2Se_3), has gained significant research interest due to its many benefits, including affordability, environmental friendliness, and stability [7,8]. It can be used as a bottom cell in a tandem solar cell or as a single-junction solar cell due to its direct bandgap, which falls in the range of (1.1–1.3 eV). Sb_2Se_3 also exhibits a high absorption coefficient and strong carrier mobility [9,10]. Recent studies have indicated that the power conversion efficiency (PCE) of Sb_2Se_3-based solar cells has rapidly increased from an initial value of less than 3 % to about 9.2 %, indicating significant potential for the material [11,12]. However, the performance stability of Sb2Se3 thin film solar cells is a critical issue that needs to be addressed. See (Table 1).

While much research has been conducted on the degradation of CdTe, CIGS, and CZTS thin film materials, the recent advancements in Sb2Se3 thin film solar cells highlight the need to investigate the

* Corresponding author.
E-mail address: nima.gorji@tudublin.ie (N.E. Gorji).

https://doi.org/10.1016/j.rinp.2023.107043
Received 27 August 2023; Received in revised form 25 September 2023; Accepted 28 September 2023
Available online 29 September 2023

Table 1
Value of simulation parameters used in amps-1d platform[19,20].

Material Properties	ITO	Cds	Sb_2Se_3
Thickness (μm)	0.050	0.050–0.060	1
Bandgap (eV)	3.3	2.4	1.08
Electron Affinity (eV)	4.5	4.2	3.7
Dielectric Permittivity	9	10	9.86
CB Effective Density of State ($1/cm^3$)	1.8×10^{18}	2.2×10^{18}	19×10^{18}
VB Effective Density of State ($1/cm^3$)	1.5×10^{19}	$2.4\ 10^{19}$	2.15×10^{18}
Electron Thermal Velocity (cm/s)	10^7	10^7	10^7
Hole Thermal Velocity (cm/s)	10^7	10^7	10^7
Electron Mobility ($cm^2/V.s$)	10^2	102	15
Hole Mobility ($cm^2/V.s$)	25	25	5.1
Donor Density (N_D) (cm^{-3})	10^{18}	1.1×10^{17}	variable
Acceptor Density (N_A) (cm^{-3})	10^{18}	0	6.78×10^{14}

Fig. 1. The schematic structure of a cds/ sb_2Se_3 thin film solar cell.

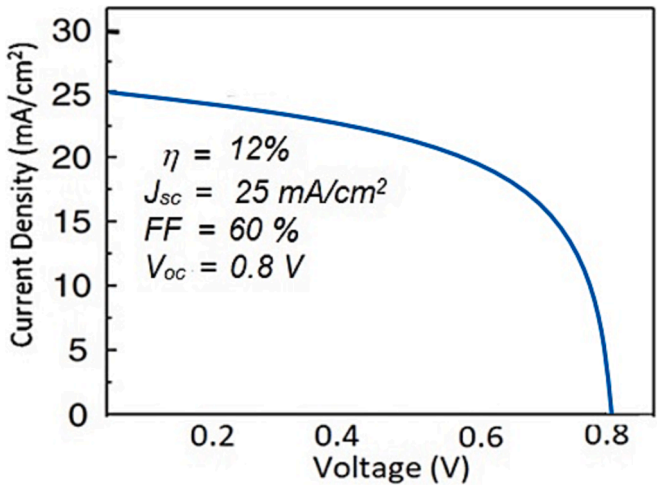

Fig. 2. Current–voltage characteristics of CdS/Sb_2Se_3 thin film solar cell with the typical value of the performance metrics. We have taken the resistance into consideration which resulted in FF = 60 % in agreement with the experimental data reported in literature [25].

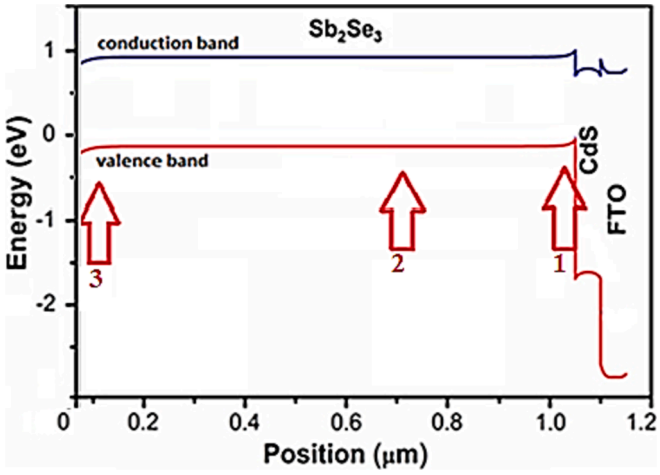

Fig. 3. The position of defect generation / accumulation at three locations at the interface, bulk and junction of sb_2Se_3 layer. The Sb_2Se_3 has been inserted in AMPS-1D platform in 3 divided layers to enable implementing the defect growth in these locations.

degradation of this type of material under operational conditions to improve their performance stability and commercialization potential [13,14]. We have previously introduced a time-dependent analysis to investigate the degradation of CdTe and CIGS thin film solar cells by developing a time-dependent modelling method and linking it to the Analysis of Microelectronics and Photonic Structures (AMPS-1D) simulation platform [15,16]. In this study, we expand our research to Sb2Se3 thin films. Our current focus is on the accumulation of defect generation at different locations within the bulk of the Sb2Se3 layer. We will demonstrate how the accumulation of defects at various thicknesses of the Sb2Se3 layer leads to a decrease in cell efficiency. Initially, we showed that the degradation was solely attributed to defect generation. However, further research has revealed that it is not only the defect concentration that matters but also their distribution within the material. The location and density of these defects play a crucial role in determining how rapidly they accumulate and ultimately lead to performance degradation. By identifying key areas of defect formation and increasing their population under operating conditions, we can prevent or slow down their accumulation and maintain optimal performance levels. Several studies have reported on the use of simulation tools such as SCAPS or AMPS to investigate defect concentration and carrier transport in Sb2Se3 thin film solar cells. These simulation tools enable the modelling of solar cell behaviour under various conditions and help identify the factors that affect its performance [17,18].

In this research paper, a time-dependent model was created to analyse defect growth in the absorber layer of Sb_2Se_3 thin film solar cells. The model was integrated with the AMPS-1D simulation platform to assess how increasing defect density at different positions within the Sb_2Se_3 layer affects the solar cell's electrical parameters. The study adopted the Gloeckler standard model for thin films in AMPS to represent Sb_2Se_3 materials and tracked the degradation of device performance parameters over time as donor-like mid-gap states accumulated in the Sb_2Se_3 layer.

Theory & simulation

This study examines the standard model of thin-film solar cells with a structure of ITO/CdS/Sb2Se3, where each layer contains a Gaussian distribution of defect density. The Sb_2Se_3 layer has been divided into three sub-layers, and the increment in defect density at each layer has

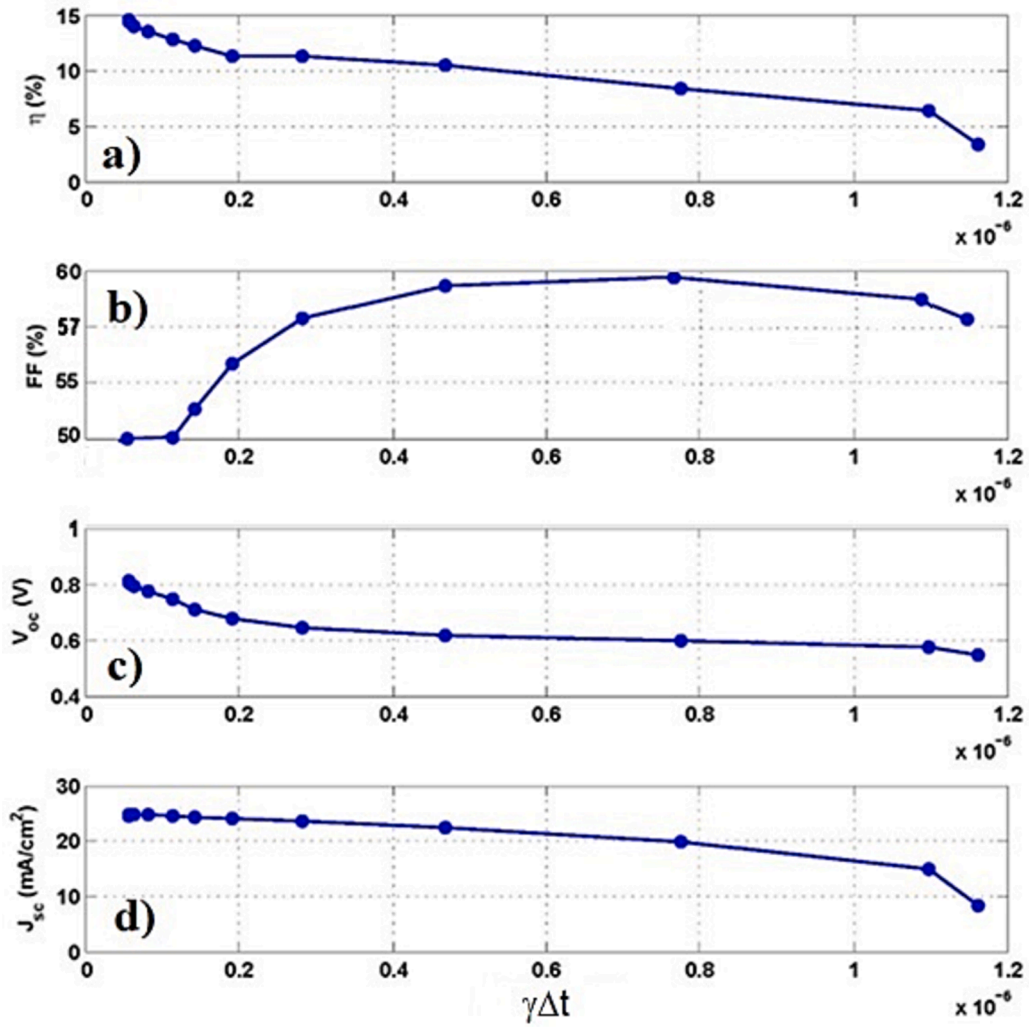

Fig. 4. The variation of electrical parameters of the cell such as a) performance, b) fill factor, c) open-circuit voltage, and d) short-circuit current density when the defect concentration at cds/sb_2Se_3 junction increases by 1.5%.

been separately investigated. The defect generation/annihilation equation will be solved together with the continuity equation to describe the dynamic process of changes in carrier concentration due to defect density. The electrical metrics of the solar cells, such as open-circuit voltage (V_{oc}), short-circuit current density (J_{sc}), fill factor (*FF*), and performance (η), will be analyzed. In Fig. 1a, the structure of the solar cell considered includes all the standard values of parameters, as found in the literature [19,20]. Fig. 1b depicts the energy diagram of the cell, with the absorbing layer divided into three sub-layers. The model presented here was well-developed by our group in the past and by the researcher in the group of Prof. Victor Karpov in the school of physics of University of Toledo, USA. It considers defect generation and annihilation as dynamic processes over time under stress or normal operational conditions, rather than static mechanisms [21,22].

Theory and modelling

In the standard model of ITO/CdS/Sb_2Se_3, each layer contains a Gaussian distribution of defect density located as donor (at 1.8 eV), acceptor (at 1.2 eV) and donor (at 0.75 eV) like defect states, respectively. In this study, the Sb_2Se_3 layer was considered as the main defective layer. Since defect generation under operation condition is a dynamic process (time-dependent), the continuity equation can be applied,

$$\frac{dN}{dt} \propto n \Rightarrow \frac{dN}{dt} = \gamma n \tag{1}$$

where *N* is the density of defect states and n is the carrier concentration. The parameter γ is the defect generation or annihilation coefficient and is dependent on deposition quality of materials in interface and bulk Sb_2Se_3 materials. In this study we set it at $\gamma = 0.8\text{x}10^{-3}$ Eq. (1) is applied to the case that the concentration of the defect is uniform throughout the absorber thickness. However, in reality, defect density is thickness dependent and might be considered position and time dependent as well e.g. in form of *N(z,t)*. The carrier concentration will change in similar way. The Eq. (1) can be written as,

$$\Delta N(z,t) = \gamma\, n\, \Delta t \tag{2}$$

It means that any small increase in the density of the defects during the time will change the carrier concentration which is in turn will influence on the performance parameters. The prediction about ΔN in a Δt will not be easy or reasonable for all the solar cells, we limit the calculations to the following estimation,

$$\Delta N = 1.5\, N_i \tag{3}$$

Ni is the initial density of defects. This limit suggests that the defect density changes by the factor 1.5 times of the prior density. Then the final density will be,

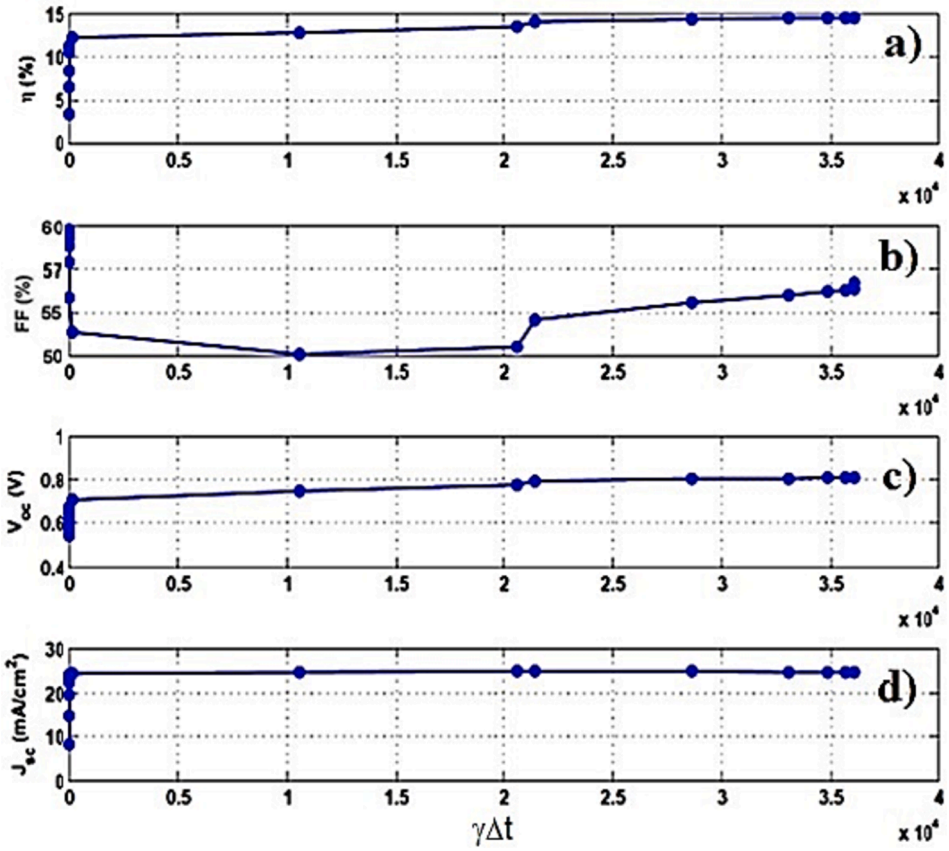

Fig. 5. The variation of the electrical parameters such as a) performance, b) fill factor, c) open-circuit voltage, and d) short-circuit current density when the defect concentration increases during the time at the middle of the Sb_2Se_3 layer in sub-layer 3.

$$N_f = \Delta N + N_i \quad (4)$$

Simulation procedure: The increment is inserted into the AMPS interface, and the electrical parameters, as well as the electron concentration (n), can be recorded using Eq. (1). At this point, we calculate the electron carrier concentration (n_f) and defect concentration (N_f) based on the initial electron density (n_i) and initial defect density (N_i) for a given $\gamma\Delta t = 1000$. We have set $\Delta t = 100$ h for this analysis in Eq. (2). Subsequently, N_f and n_f are input into AMPS-1D at various locations within the Sb2Se3 layer, and the program is iteratively run to observe significant changes in the current–voltage characteristics and overall cell performance. Table I presents the parameter values used in this simulation study.

The structure of the CdS/Sb_2Se_3 solar cell has already been implemented in the AMPS platform, and reference parameters have been generated to ensure that the solar cell is operating under proper conditions before introducing the secondary concentrations of electrons and defects. The initial current–voltage characteristics of the cell are provided in Fig. 2. The values of N_f and n_i are inserted at three different positions within the Sb_2Se_3 layer using AMPS-1D, as indicated by arrows in Fig. 3. Layers 2 and 3 exhibit similar carrier transport properties, so we focused on defect/electron accumulation in layer 3 and ensured that this would have the same effect on layer 2. As carrier and defect concentrations change continuously from the interface of the Sb_2Se_3 layer to the back contact, it is advisable to track this variation point by point [23,24]. However, in some thickness intervals, these changes are minimal, so we have recorded data at only three points within absorber layer, as shown in Fig. 3. The defect density at the interface between front-contact and back-contact electrodes with Sb_2Se_3 were set at $3.12\text{x}10^{17}$ cm^{-3}.

Results & discussion

The objective here is to observe the variation in η, FF, V_{oc}, and J_{sc} over time under prolonged irradiation during normal operational conditions at 100 mW/cm^2, resulting in an increase in defect density. The simulation has been conducted using AMPS-1D, employing the Gloeckler standard model adapted for Sb_2Se_3 material. Optical, electrical, and materials properties of the Sb_2Se_3 layer have been input into the AMPS platform, and the Sb_2Se_3 layer has been divided into three sub-layers to help us understand which part of the cell is more susceptible to degradation and more sensitive to defect generation and accumulation. Donor-like mid-gap states have been activated in AMPS, and the program is iteratively run to obtain updated performance metrics after increasing the defect density at a specific position.

Fig. 4 illustrates the variation in device metrics with increasing degradation time, which is equivalent to the increment in defects after 100 h of stressing the device. Even a slight increase in defect density in the mid-gap level for different time intervals leads to a significant drop in performance parameters. Therefore, we obtained the variation in electrical parameters such as V_{oc} and J_{sc} over time using Eq. (1) with the assistance of AMPS iterations. When ΔN changes by $1.5N_i$, with Ni initially set at $10\text{x}10^{12}$ cm^{-3}, the defect distribution at three points at 0.525 μm (at the very interface of CdS/Sb_2Se_3), 3.68 μm (in the middle of the Sb2Se_3 layer), and 4.62 μm (at the back contact) differs. In each iteration, N and carrier concentration (n) values are recorded in the AMPS interface, and $\gamma\Delta t$ is calculated using Eq. (1).

The electrical parameter changes are presented in the following results. When the defect increment occurs at the CdS/Sb_2Se_3 interface, the efficiency decreases sharply initially and then at a slower rate over longer time intervals. The change in the parameters during the initial intervals is more pronounced compared to the later ones. The fill factor

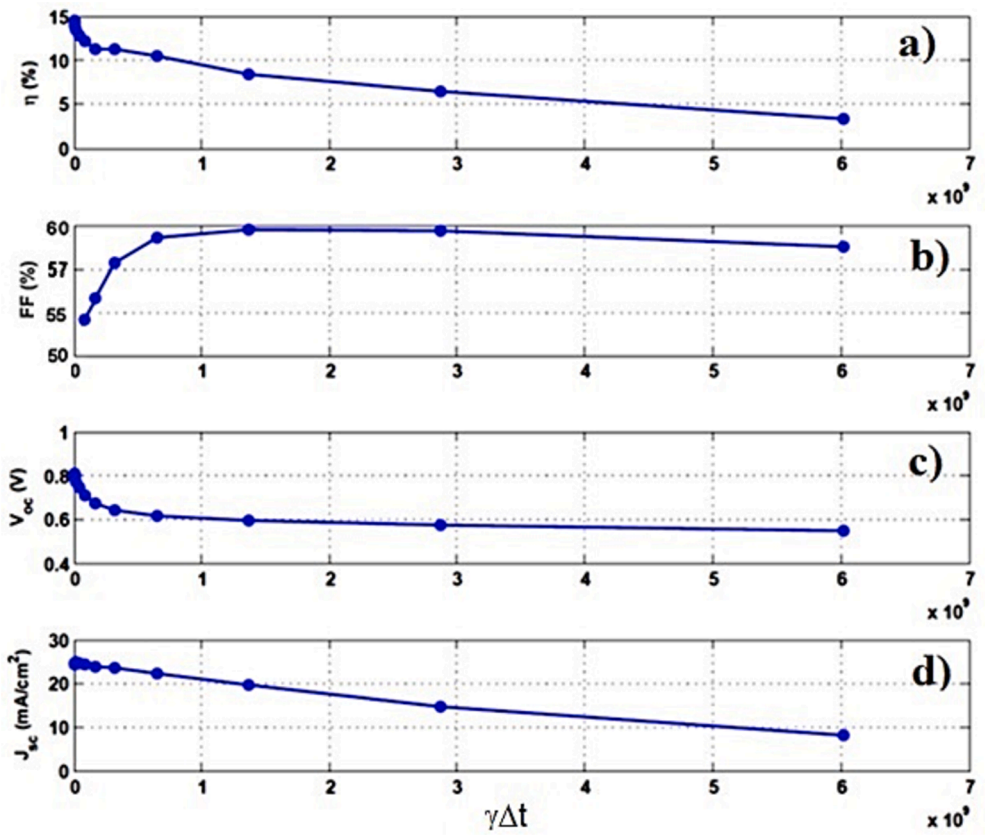

Fig. 6. The variation of the electrical parameters such as a) performance, b) fill factor, c) open-circuit voltage, and d) short-circuit current density over the time when the defect concentration increases at the junction of Sb_2Se_3 layer and metallic electrode.

(*FF*) exhibits a rapid decline initially, followed by reaching a constant and optimum value. The presence of defect states alters the space charge characteristics of the cell in a manner like interface states.

When the defect density increases in the middle of the Sb_2Se_3 layer (sublayer 3 as shown in Fig. 3), the electrical parameters vary as depicted in Fig. 5. In this case, the efficiency begins to decrease over longer periods, and it reduces more rapidly over shorter time intervals. Consequently, the defect density in the middle of the Sb_2Se_3 layer can decrease efficiency over longer durations, while the rapid increment of defects leads to efficiency reduction within shorter time frames. This explains why efficiency is lower for smaller $\gamma\Delta t$ and increased N, as shown in the left part of the results in Fig. 5.

Finally, the variation in electrical parameters over time is depicted in Fig. 6, where the defect density increases at the end of the Sb_2Se_3 layer where the junction with the electrode is sensitive to defect growth and accumulation and can hinder the hole passivation and electron's flow through the absorbing layer to electrode.

In Fig. 6, the variation in defect concentration over time at three different points within the absorber layer and metallic electrode is displayed. This figure illustrates the change in electrical parameters over time as the defect concentration increases at the end of the absorber layer, demonstrating the impact of defect concentration on the performance of the photovoltaic device. As the defect concentration increases, the generation/recombination rate may be affected, leading to a decline in the device's efficiency. This decline is evident in key electrical parameters such as short-circuit current (J_{sc}), open-circuit voltage (V_{oc}), fill factor (*FF*), and conversion efficiency. Additionally, there is an increase in series resistance (R_s) and a decrease in shunt resistance (R_{sh}) with the increasing defect concentration.

The variation of the n carrier concentration against time at three different positions of the absorber layer is shown in Fig. 7. it is likely that there will be a variation in defect concentration over time at different points within the absorber layer. The accumulation of impurities and defects may be highest at the junctions between different layers, such as the ITO/CdS or CdS/ Sb_2Se_3 interfaces [22–24]. These areas may experience the highest levels of stress, such as temperature and light soaking, leading to increased defect concentration and degradation over time. In contrast, areas deeper within the absorber layer may have lower defect concentrations, as they are less exposed to external stressors. The exact variation of defect concentration over time will depend on the specific materials and manufacturing processes used in the production of the thin film solar cells.

Other parameters also influence the results mentioned above. For instance, the balance between the carrier cross-sections, σ_n and σ_p, can impact the space charge of the absorber layer near the interface, leading to a shift in the Fermi levels. This, in turn, can control the effect of defect densities. A similar mechanism can be predicted for the acceptor and donor concentrations in the absorber and window layers, respectively. As illustrated in Fig. 8, when studying the increase in defect density, attention should be paid to the concentrations of N_A and N_D in the cell layers. The concentration of impurities can affect the generation/recombination rate and cause degradation over time. Impurities can be induced or accumulated at the junction, and examples of impurities that cause degradation include Cl_S-V_{Cd}, Cu_{Cd} complexes, and those with a density of 10^{18}-10^{20} cm^{-3} at TCO/CdS or CdS/Sb_2Se_3 interfaces.

What is evident in Figs. 7 and 8 is that when the concentration of recombination centers changes, the efficiency variation is sharp during the initial time intervals, but it slows down in subsequent times. Furthermore, these results indicate that the variation in defect density is not uniform throughout the absorber thickness; it is more probable at the junction and around the space charge region (SCR). The variation in V_{oc} at the junction (Fig. 5) reaches the lowest value (<0.5 V), while the minimum V_{oc} at the end of the absorber layer is 0.6 V. This suggests that V_{oc} does not change uniformly across the cell because of the stronger

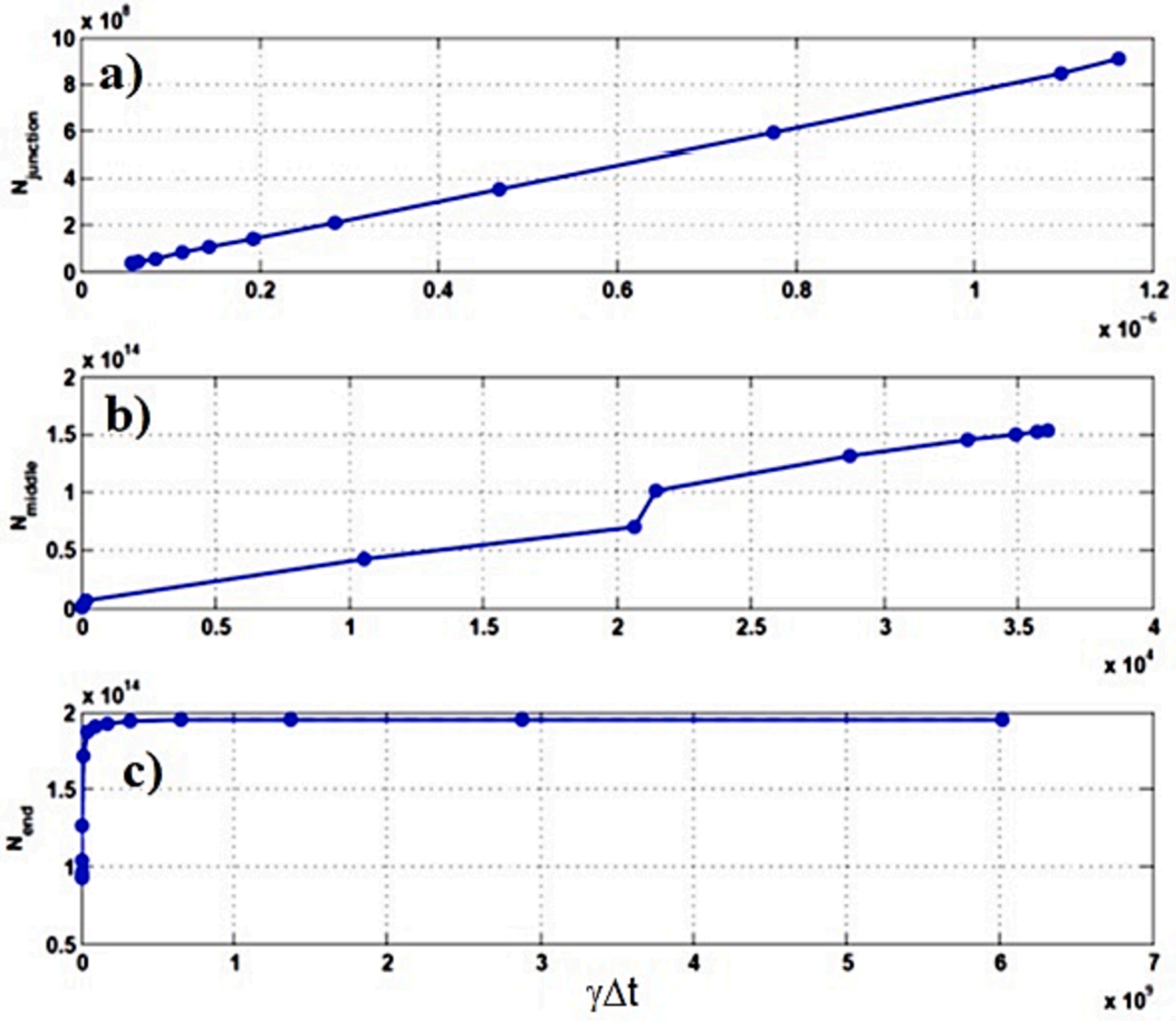

Fig. 7. The variation of the defect concentration versus time at three different points of the absorber layer a) at the junction of cds/sb_2Se_3, b) the middle layer in bulk of Sb_2Se_3 layer, and c) at the junction of Sb_2Se_3 and metallic electrode.

effect of recombination centers at the junction over time. The variation in V_{oc} appears to have a slight distribution throughout the thickness. In all cases, the variation in *FF* is less than 10 %. There is a cliff for *FF* at the junction, possibly because increasing the defect density in the junction reduces the SCR and decreases the recombination lifetime, resulting in higher recombination at the junction and a lower *FF*. However, *FF* increases later and reaches a constant value. In this case, the high density of defect density becomes comparable with the acceptor concentration in the absorber layer, reducing the recombination rate and increasing the *FF*.

Correlation of simulation and experimental data

We acknowledge the importance of calibrating our simulation with experimental data to build confidence in our modeling results. It is important to note that modeling the degradation trend of solar cells with lower than 10 % performance is not sensible for researchers. We have identified literature where the drop in performance parameters agrees well with our modeling results. Wen et al. reported over 5 % drop in performance of Sb_2Se_3 solar cells at higher temperatures [25]. This is in agreement with the degradation trend in Fig. 4 where the performance of the cell drops from 15 % to about 10 % in the initial stages of defect growth at the interface of Sb_2Se_3 layer. We assign this to a strong value of electric field weakening at the p-n junction upon defect growth under stress which impacts on carrier transport at the interface. In a separate study by Hu et al., the drop in current and voltage of the cell was five times upon stressing the cell under heat and temperature elevation to over 325 K [26]. This is in agreement with our study as in Fig. 6 we observed a decrease in V_{oc} from 0.8 V to lower around 0.5 V which is due to increased defect growth at the bulk of the cell where the defect increase can impede the smooth drift or diffusion of electrons and holes.

Kumari et al. presented SCAPS-1D modeling of the Sb_2Se_3 solar cells and realized over 0.8 V open-circuit voltage due to use of NiO as the hole-transporting layer [27]. Mamta et al. have also presented $MoSe_2$ back surface layer to significantly increase the open-circuit voltage of Sb_2Se_3 solar cell [28]. which is in line with our results in Figs. 4-6 where the V_{oc} could rise to over 0.8 V if we continue the defect generation rate.

Conclusion

A time-dependent modeling method has been developed to investigate the degradation of performance parameters of Sb_2Se_3 thin film solar cells by increasing the defect density at three different positions within the Sb_2Se_3 layer (at the interface with CdS, in the bulk of the Sb_2Se_3

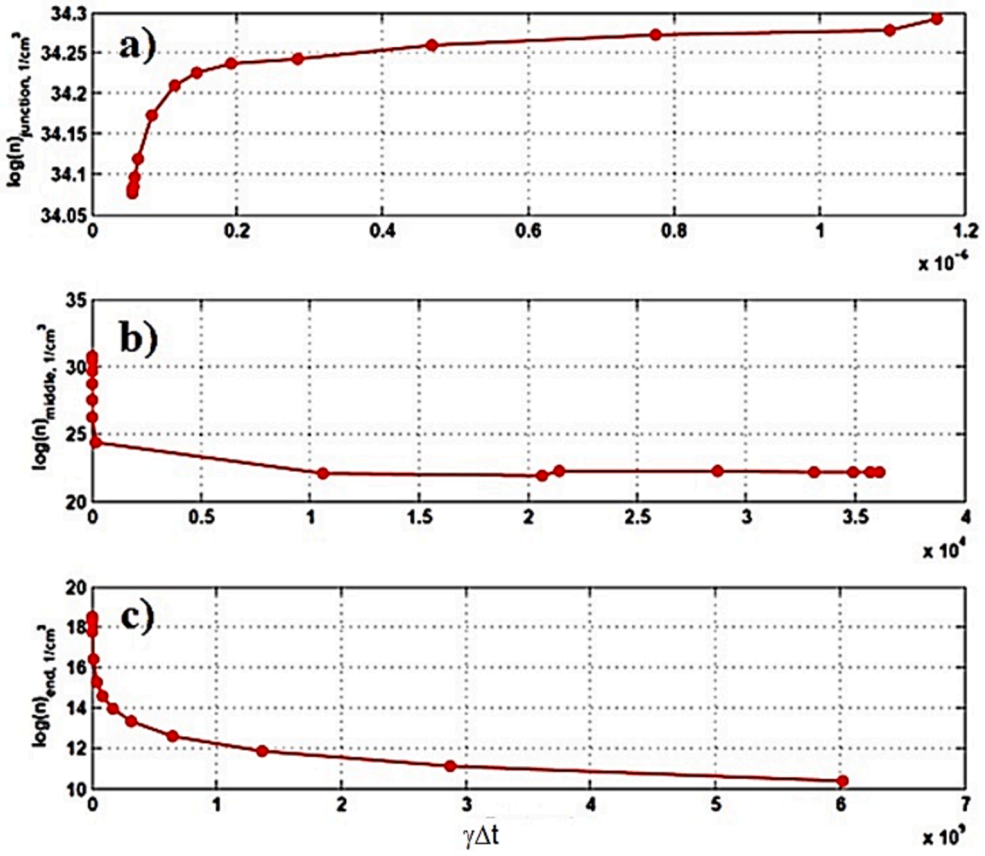

Fig. 8. Variation of the n, carrier concentration against time at three different positions of the absorber layer: a) at the junction of cds/sb_2Se_3, b) the middle layer in bulk of Sb_2Se_3 layer, and c) at the junction of Sb_2Se_3 and metallic electrode.

layer, and at the interface with the top contact). This time-dependent model was developed and linked to the AMPS-1D platform to investigate the increment of defects within the mid-gap of Sb_2Se_3. The simulation analysis emphasizes changes in the electrical parameters of a solar cell due to an increase in defect density, utilizing the Gloeckler standard model for Sb_2Se_3 materials within the AMPS platform. The variation of η, *FF*, *Voc*, and J_{sc} with respect to time is tracked at three different points within the absorber layer. An increase in defect density results in changes in carrier and defect concentrations, which are recorded using Eq. (1) and $\gamma\Delta t$. The efficiency of the cell decreases sharply at the beginning and then gradually over time if the defect increment occurs at the CdS/Sb_2Se_3 interface. The FF exhibits a sharp decline initially, followed by stabilizing at an optimum constant value. The presence of defect states alters the space charge within the cell similarly to interface states. Changes in solar cell efficiency are attributed to the concentration of recombination centers, affecting V_{oc} and *FF*. The efficiency variation is pronounced initially and then slows down. The variation in defect density is not uniform throughout the absorber thickness, being more pronounced at the junction and around the space charge region. V_{oc} varies unevenly across the cell due to the stronger influence of recombination centers at the junction over time, showing slight distribution through the thickness. *FF* displays a cliff at the junction but subsequently increases and reaches a constant value. A high density of defect density becomes comparable to the acceptor concentration within the absorber layer, reducing the recombination rate and increasing *FF*.

CRediT authorship contribution statement

Ming-Lang Tseng: Formal analysis, Simulations, Investigation. **Malek Gassoumi:** Formal analysis, Investigation, Writing – original draft. **Nima E. Gorji:** Conceptualization, Data curation, Formal analysis, Investigation, Supervision, Writing – original draft, Writing – review & editing.

Declaration of Competing Interest

The authors declare that they have no known competing financial interests or personal relationships that could have appeared to influence the work reported in this paper.

Data availability

No data was used for the research described in the article.

References

[1] Theelen M, Hagedoorn C, Neugebohrn N. Damp heat induced degradation mechanisms occurring in colored oxide/metal/oxide films for thin-film solar cells. Thin Solid Films 2021;138711:730.
[2] Mishra Sh, Bhargava K, Deb D. Numerical simulation of potential induced degradation (PID) in different thin-film solar cells using SCAPS-1D. Sol Energy 2019;188:353–60.
[3] Yang Ch, Song K, Wu Zh. Strain dependent effect on power degradation of CIGS thin film solar cell. Sol Energy 2020;195:121–8.
[4] GhoshM S, MoreiraJ VB, González C. Growth and optical properties of nanocrystalline Sb_2Se_3 thin-films for the application in solar-cells. Sol Energy 2020; 211:613–21.
[5] Aliyar M, Arumukham F, Bandara MJ. Recent advances and new research trends in Sb_2S_3 thin film based solar cells. J Sci: Adv Mater Devices 2023;8(1):100533.
[6] Marwa A, Salem S, Jayan D. Analysis and design of p-n homojunction Sb_2S_3 solar cells by numerical simulation. Sol Energy 2022.
[7] Liang G, Liu T, Ishaq M, Chen Z, Tang R, Zheng Z, et al. Heterojunction interface engineering enabling high onset potential in Sb2Se3/CdS photocathodes for efficient solar hydrogen production. Chem Eng J 2022;431(3):133359.
[8] Luo Y-D, Tang R, Chen S, Hu J-G, Liu Y-K, Li Y-F, et al. An effective combination reaction involved with sputtered and selenized Sb precursors for efficient Sb_2Se_3 thin film solar cells. Chem Eng J 2020;393:124599.

[9] Chen C, Lu S, Zeng K, Yang B, Gao L, Prof J, et al. Characterization of basic physical properties of Sb_2S_3 and its relevance for photovoltaics. Front Optoelectron 2017; 10:18–30.
[10] Luo Y, Chen G, Chen S, Ahmad N, Azam M, Zheng Z, et al. Carrier transport enhancement mechanism in highly efficient antimony selenide thin-film solar cell. Adv Funct Mater 2023;33(14):2213941.
[11] Luo Y-D, Tang R, Chen S, Hu J-G, Liu Y-K, Li Y-F, et al. An effective combination reaction involved with sputtered and selenized Sb precursors for efficient Sb2Se3 thin film solar cells. Chem Eng J 2020;393(1):124599.
[12] Miao Luo; Meiying Leng; Xinsheng Liu; Jie Chen; Chao Chen; Sikai Qin; Jiang Tang, Thermal evaporation and characterization of superstrate CdS/Sb2Se3 solar cells. Appl. Phys. Lett. 104, 173904 (2014).
[13] Liang G, Chen M, Ishaq M, Li X, Tang R, Zheng Z, et al. Crystal growth promotion and defects healing enable minimum open-circuit voltage deficit in antimony selenide solar cells. Adv Sci 2022;9(9):2105142.
[14] Chen S, Fu Y, Ishaq M, Li C, Ren D, Su Z, et al. Carrier recombination suppression and transport enhancement enable high-performance self-powered broadband Sb2Se3 photodetectors. Infomat 2023;5(4):e12400.
[15] Gorji NE, Reggiani U, Sandrolini L. Numerical analysis of degradation kinetics in CdTe thin films. Sol Energy 2015;118:611–21.
[16] N. E. Gorji; U. Reggiani; L. Sandrolini, Peculiar Role of Holes and Electrons in the Degradation of CdTe Thin Films, IEEE Transactions on Device and Materials Reliability, 15:2, (2015) 198-205.
[17] Md. F. Rahman, Md. Moon, …, A. B. Md. Ismail, Concurrent investigation of antimony chalcogenide (Sb2Se3 and Sb2S3)-based solar cells with a potential WS2 electron transport layer *Heliyon,* 8:12 (2022) 12034.
[18] Maurya M, Singh V. Sb_2Se_3/CZTS dual absorber layer based solar cell with 36.3% efficiency: a numerical simulation. J Sci: Adv Mater Devices 2022;7(9):100445.
[19] Basak A, Singh UP. Numerical modelling and analysis of earth abundant Sb_2S_3 and Sb_2Se_3 based solar cells using SCAPS-1D. Sol Energy Mater Sol Cells 2021;230: 111184.
[20] Harju R, Karpov VG, Grecu D, Dorer G. Electron-beam induced degradation in CdTe photovoltaics. J Appl Phys 2000;88(4):1794–800.
[21] Karpov VG, Compaan AD, Shvydka D. Effects of nonuniformity in thin-film photovoltaics. Appl Phys Lett 2002;80(22):4256–60.
[22] Yuan C, Jin X, Jiang G, Liu W, Zhu C. Sb2Se3 solar cells prepared with selenized dc-sputtered metallic precursors. J Mater Sci Mater Electron 2016;27:8906–10.
[23] Lin J, Chen G, Ahmad N, Ishaq M, Chen S, Su Z, et al. Back contact interfacial modification mechanism in highly-efficient antimony selenide thin-film solar cells. Journal of Energy Chemistry 2023;80:256–64.
[24] Tang R, Chen S, Zheng Z-H, Su Z-H, Luo J-T, Fan P, et al. Heterojunction annealing enabling record open-circuit voltage in antimony triselenide solar cells. Adv Mater 2022;34(14):2109078.
[25] Wen X, Chen C, Lu S, Li K, Kondrotas R, Zhao Y, et al. Vapor transport deposition of antimony selenide thin film solar cells with 7.6% efficiency. Nat Commun 2018;9: 2179.
[26] Hua X, Taoa J, Wanga Y, Xuea J, Wenga G, Zhang C, et al. 5.91%-efficient Sb2Se3 solar cells with a radio-frequency magnetron-sputtered CdS buffer layer. Appl Mater Today 2019;16:367–74.
[27] Kumari R, Mamta AK, Chaudhary VN. Performance analysis of CdS-Free, Sb_2Se_3/ZnSe p–n junction cells with various hole transport layers and contacts. Advanced Theory and Simulations 2023:2300322. https://doi.org/10.1002/adts.202300322.
[28] Mamta M, Kumari R, Maurya KK, Singh VN. Performance of Sb_2Se_3-based solar cell: with and without a back surface field layer. Energ Technol 2023;11(6): 2201522. https://doi.org/10.1002/ente.202201522.